

Determination of Material Thicknesses in Protective Clothing for Firefighters

DOI: 10.5604/01.3001.0011.5745

Lodz University of Technology,
Faculty of Material Technologies and Textile Design,
Department of Technical Mechanics
and Computer Science,
Lodz, Poland
E-mail: ryszard.korycki@p.lodz.pl

Abstract

The basic protective clothing for firefighters does not contact the flame and provides a relatively short exposure time to heat flux of prescribed density. Simultaneously the structure is subjected to sweat diffusion from the skin. The problem is determined mathematically by means of second-order differential equations accompanied by a set of boundary and initial conditions. Determination of the material thicknesses is gradient oriented. The optimal thicknesses are determined as a numerical example.

Key words: heat transport, moisture transport, material thickness, clothing for firefighters.

Nomenclature

A matrix of thermal conduction coefficients, $W/(m K)$,
b vector of material thicknesses, m ,
C; C_0 constraint functional and imposed constant value of constraints,
c volumetric heat capacity, $J/(kg K)$,
D matrix of mass transport coefficients, m^2/s ,
 $\text{div}_{\Gamma} \mathbf{v}^p$ tangent divergence of vector \mathbf{v}^p on external boundary Γ ,
E, G objective functional, objective functional of particular physical interpretation,
 $g_p = DG/Db_p$ global (material) derivative of g in respect of design parameter b_p ,
 $g^p = \hat{\partial}g/\hat{\partial}b_p$ partial (local) derivative of g in respect of design parameter b_p ,
H mean curvature of external boundary Γ , $1/m$,
 h, h_w heat and mass convection coefficients, $W/(m^2 K)$, m/s ,
n unit vector normal to external boundary Γ , directed outwards to domain Ω bounded by this boundary),
P number of design parameters,
q vector of heat flux density, W/m^2 ,

\mathbf{q}_w vector of mass flux density, $kg/(m s)$,
 $q_n = \mathbf{n} \cdot \mathbf{q}$ heat flux density normal to external boundary, W/m^2 ,
 $q_{nw} = \mathbf{n} \cdot \mathbf{q}_w$ mass flux density normal to external boundary, $kg/(m s)$,
 $R_1; R_2$ sorption rates during first- and second-stage of sorption, $kg/(m^3 s)$,
 R_f mean radius of fibres, m ,
 R_v specific gas constant of water vapour related to molar mass, $J/(kg K)$,
T temperature, $K/^{\circ}C$,
t real time in primary and additional structures, s ,
 t_{eq} time to reach quasi-equilibrium during sorption process, s ,
u unit cost of the structure, –
 $\mathbf{v}^p(\mathbf{x}, \mathbf{b}, t)$ transformation velocity field associated with design parameter b_p ,
 $\mathbf{v}_n^p = \mathbf{n} \cdot \mathbf{v}^p$ transformation velocity normal to external boundary Γ ,
 w_a water vapour concentration in air filling interfibre void spaces, kg/m^3 ,
 w_f water vapour concentration within fibres, kg/m^3 ,
 W_c fractional water content on fibre surface,
x coordinate vector of crucial geometrical points, m ,
 Γ external boundary of structure,
 ε effective porosity of textile material,
 κ emissivity of surfaces subjected to heat radiation,
 σ Stefan-Boltzmann constant, $W/(m^2 K^4)$,
 λ_w cross transport coefficient, i.e. heat of sorption of water vapour by fibres, J/kg ,
 Σ discontinuity line between adjacent parts of piecewise smooth boundary Γ ,
 ρ density of fibres, kg/m^3 ,
 χ Lagrange multiplier,
 Ψ, γ domain and boundary integrands of objective functional,
 Ω structural domain, m^2 ,
 ∇ gradient operator.

Introduction

The light/basic protective clothing for firefighters does not contact the flame and provides a relatively short exposure time to the heat flux of the prescribed density. The impermeable layer/membrane ensures the diffusion of sweat from the skin and prevents the transport of water vapour from the surroundings. The air gaps within the clothing provide additional heat insulation to the user.

The effect of coupled transport on the protective performance of a garment was investigated by Chitrphiromsri and Kuznetsov [1]. However, the model fire – fabric – air gap – skin system applied is different from that introduced in the work presented. A numerical model of heat and moisture transport in protective clothing during exposure to a flash fire was introduced by Song, Chitrphiromsri & Ding [2]. The influence of air gaps as well as convectional and radiation heat transfer were comprehensively discussed. A general model of coupled transport and interaction with human comfort were investigated by Li [3]. Some solutions proposed introduce additional air layers inside the garment, which are created by active elements. The effect of additional layers on thermal insulation was analysed by Ghazy and Bergstrom [4, 5]. Heat transported from the source to the skin can be partially absorbed by phase change materials, cf. Fan, Chen [6]. Different Authors introduce processing variables to determine an optimal structure made of specified materials [7]. The models applied depend on the type of clothing for firefighters. Song et al. [8] introduce a model for low radiant heat protection, whereas Rossi et al. [9] present a model of the flame engulfment test. The effect of moisture transport on protective clothing exposed to insignificant heat flux was discussed by Barker et al. [10].

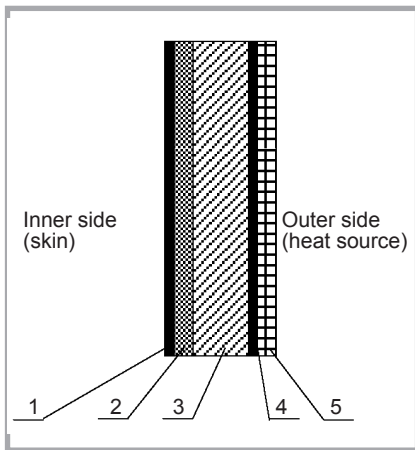


Figure 1. Cross-section of basic protective clothing for firefighters: 1 – inner blocking layer, 2 – lining, 3 – non-woven layer, 4 – impermeable membrane, 5 – external fabric.

Selected aspects of coupled transport were described by some authors. Combined moisture sorption, condensation and liquid diffusion was introduced by Li & Zhu [11]. The coupled model gives an approximate solution and its variational form is difficult to define, cf. Li & Luo [12]. The same authors describe a diphasic model of the sorption process within fibres. Optimisation of material thicknesses is typical for textile structures and is determined by a low number of design variables. The isogeometric approach to shape optimisation was discussed by Wang, Turteltaub & Abdalla [13] and Wang & Kumar [14]. Effective thermal conductivities in gradient materials were discussed by Turant [15] and Turant & Radaszewska [16].

The paper is a continuation of previous analyses concerning the determination of state variables within complex composites, cf. [17, 18]. The shape optimisation of textile composites subjected to coupled heat and mass transport was discussed in [19, 20] using the material derivative concept and first-order sensitivities. Textile structures can also be optimised in respect of moisture transport, cf. [21].

The character and shape of a textile structure are determined by geometrical dimensions as well as physical, strength and physiological properties. The problem is described by the vector of structural parameters, which can be structural topology, cross-sectional shapes, material type and weight, as well as physical, chemical and mechanical properties. Some additional parameters can be de-

scribed using fuzzy logic. Thus optimisation is a multidisciplinary problem which is defined by the complex objective functional of unequivocal physical interpretation (assuming the variational approach to sensitivity analysis). The procedure proposed is considerably limited to shape optimisation, that is the optimisation of geometrical dimensions in respect of the physical properties prescribed.

The main goal of the paper is to determine the optimal material thicknesses in basic protective clothing for firefighters. The heat insulation and structure of protective clothing can be improved by means of additional air gaps which are created by shape memory elements at the prescribed temperature. Thus numerical optimisation is always cheaper and gives more general results than the practical tests, with measurable numerical and economic benefits.

The novelty elements are the following: (i) introduction of additional void spaces between the material layers, which are created by shape memory elements at the prescribed temperature. (ii) description of physical phenomena and formulation of different boundary conditions for the initial shape and activated memory elements within the clothing. (iii) determination of optimal material thicknesses in respect of the slowest moisture and heat transport through the material and void layers.

Modelling of coupled transport within protective clothing

The basic protective clothing for firefighters is exposed to radiation heat transport from external sources and sweat/moisture diffusion from the skin. This type of clothing should not contact the flame. The resistance of basic protective clothing to radiant heat is determined for the reference materials according to EN-ISO 6942: 2002 [22]. The material is exposed to thermal radiation of heat flux density $q_n = (20-40) \text{ kW/m}^2$. The time of a temperature rise of $12 \text{ }^\circ\text{C} / 24 \text{ }^\circ\text{C}$ is recorded and defined as $RHTI_{12}/RHTI_{24}$, respectively. The level of heat insulation depends on the class of protective clothing and time of the temperature rise; $RHTI_{24} \geq 10 \text{ s}$ for protection class 1, and $RHTI_{24} \geq 18 \text{ s}$ for protection class 2. Thus heat flux density $q_n = 20 \text{ kW/m}^2$ requires maximal values $50 \text{ s} \geq RHTI_{24} \geq 20 \text{ s}$. It follows that the time of effective work in

basic protective clothing should not exceed several minutes.

Human sweat is fluid and consists of water (about 98%), NaCl (0.6-0.8)%, fat, urea, uric acid, ammonia etc. Thus we introduce the diffusion of water vapour because the content of other ingredients is negligible. The physiology of sweat secretion is an individual characteristic feature and depends on personal differences, temperature level, stress, physical activity, etc.

Let us assume a complex structure made of several textile layers subjected to heat and mass transport, as in **Figure 1**. The shape and boundary conditions are repeatable within the clothing and the spatial problem is reduced to any cross-section. The incombustible external fabric is made of aramid fibres, for example Nomex, Kevlar or Kelmar. Moisture transport from the skin to the surroundings is blocked by the semipermeable membrane. The non-woven layer improves thermal insulation and absorbs moisture. The incombustible lining is an additional absorbing and insulating layer. The inner barrier is the textile layer, which absorbs sweat and partially prevents the returnable penetration of moisture into the skin.

A textile structure consists of fibres and void spaces between textile material. However, fibres are non-homogeneous and produced by spinning from short natural filaments. Single fibres are consequently porous. The void spaces inside and between fibres are filled with air and next with sweat/water vapour. Homogenisation using the “rule of mixture” should be a two-stage process, where the fibres are homogenised during the “micro” process and then the particular layer during “macro” homogenisation.

Let us introduce the following physical assumptions: (i) Heat is transported by conduction within fibres and convection from the outer surfaces to void spaces as well as within these spaces. Mass is transported within fibres and interfibre spaces by diffusion [3, 11, 12]. (ii) Volume increase caused by mass diffusion can be neglected. (iii) Orientation of fibres can be significant although the diameters are small, and water vapour is transported through interfibre spaces faster than within fibres. The weaves are different in woven fabrics, knitted fabrics and non-wovens, and the textile structure should always be deeply

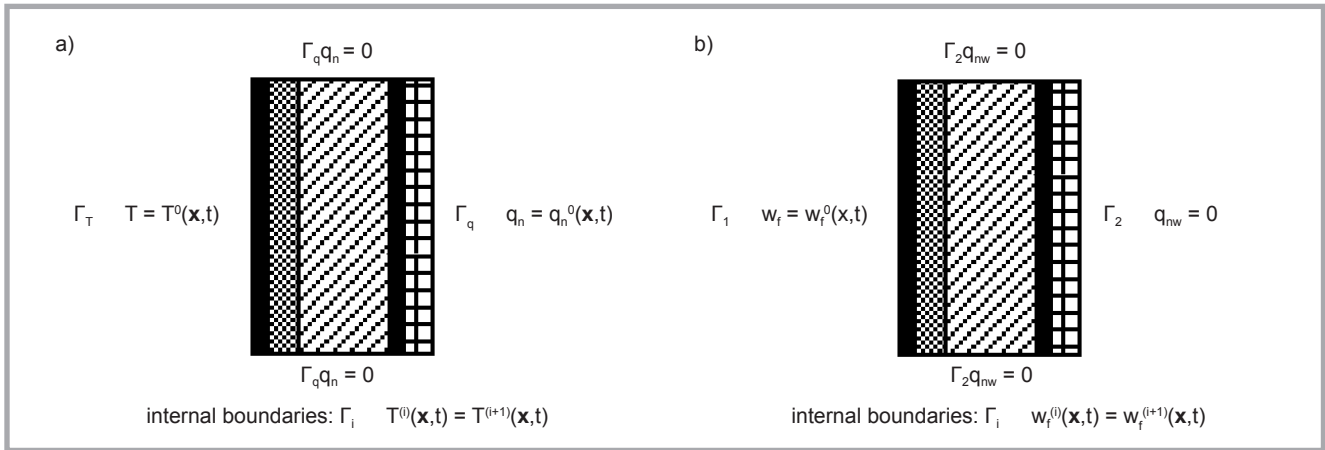


Figure 2. Boundary conditions of protective clothing for firefighters without air gaps: a) heat transport. b) moisture transport.

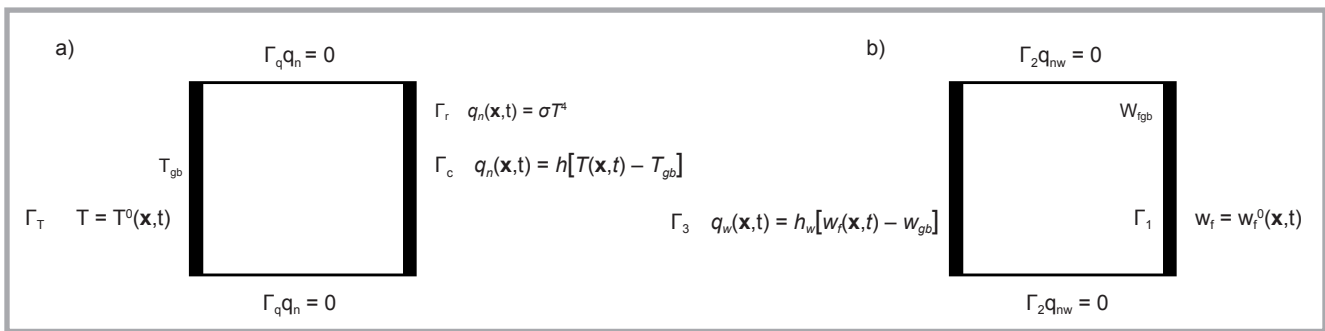


Figure 3. Boundary conditions of protective clothing within air gaps: a) heat transport, b) moisture transport. Note: T_{gb} – temperature on gap boundary; w_{gb} – water vapor concentration on gap boundary.

analysed. (iv) Although coupled transport is a disequilibrium process, instantaneous thermodynamic equilibrium can be introduced between the textile material and fluid in free spaces irrespective of time characteristics. Thus the textile fibres have small diameters and a large surface/volume ratio.

Heat and mass balances are introduced in [19, 20] for the i -th layer. Equation (1)

The third equation describes the current status of moisture sorption/desorption between fibres and interfibre spaces [3, 12]. The first stage of the sorption process is described by Fick's law and the constant diffusion coefficient of the material. Moreover Li & Luo [12] and Li [3] describe the sorption/desorption within some materials of strongly hygroscopic properties (cf. wool) using Fick's law during the entire process. Because of the short working time, the problem can be described by the first phase of the sorption. The discrete relations have the following form. Equation (2)

The equilibrium time t_{eq} is determined experimentally for different materials

and is equal to (540–600) s, cf. Li & Luo [12] and Haghi [23]. Sorption during the first phase R_1 is defined by moisture transport within dry cylindrical fibres [3, 12] according to Fick's diffusion. Equation (3)

Let us introduce the boundary and initial conditions during heat transport, Figure 2.a. The external boundary portion Γ_q is subjected to heat flux density from a heat source of arbitrary distribution in time, where heat is transmitted unidirec-

$$\begin{cases} (1 - \varepsilon^{(i)}) \frac{dw_f^{(i)}}{dt} + \varepsilon^{(i)} \frac{dw_a^{(i)}}{dt} = -\text{div} \mathbf{q}_w^{(i)}; & \mathbf{q}_w^{(i)} = \mathbf{D}^{(i)} \cdot \nabla w_f^{(i)}; \\ \rho^{(i)} c^{(i)} \frac{dT^{(i)}}{dt} + \lambda_w^{(i)} (1 - \varepsilon^{(i)}) \frac{dw_f^{(i)}}{dt} = -\text{div} \mathbf{q}^{(i)}; & \mathbf{q}^{(i)} = \mathbf{A}^{(i)} \cdot \nabla T^{(i)}; \end{cases} \quad (1)$$

$$\begin{aligned} \frac{dw_f^{(i)}}{dt} &= R_1 \quad \text{for } W_c^{(i)} < 0,185 \text{ and } t < t_{eq}; \\ \frac{dw_f^{(i)}}{dt} &= \frac{1}{2} R_1 + \frac{1}{2} R_2 \quad \text{for } W_c^{(i)} \geq 0,185 \text{ and } t < t_{eq}; & W_c^{(i)} &= \frac{w_f^{(i)}(\mathbf{x}, R_f, t)}{\rho}. \\ \frac{dw_f^{(i)}}{dt} &= R_2 \quad \text{for } t > t_{eq}. \end{aligned} \quad (2)$$

$$\frac{dw_f^{(i)}}{dt} = R_1(\mathbf{x}, t) = \frac{1}{r} \frac{d(r \mathbf{D}^{(i)} dw_f)}{dr^2}. \quad (3)$$

Equations (1), (2) and (3).

tionally. Therefore the heat flux densities are equal to $q_n = 0$ on the side boundary portions Γ_q . Let us assume that the internal boundary portion Γ_T does not contact the skin. Temperature within the void layer is time-dependent according to the prescribed function. The fourth-kind condition defines the same state variables on the common internal boundaries Γ_i without air gaps. The void spaces created by shape memory elements are characterised by the combined boundary conditions, **Figure 3.a**. The boundary portion close to the heat source is characterised

by the radiation condition and convection condition (that is, the third-kind condition) and denoted as $\Gamma_C \cup \Gamma_r$. The boundary Γ_T close to the skin is defined by the current temperature, that is by the first-kind condition.

The external boundary portion Γ_2 is protected by the membrane and external incombustible fabric, **Figure 2.b**. This is equivalent to the second-kind boundary condition on part Γ_2 of the moisture flux density equal to $q_{mw} = 0$. Moisture is transported unidirectionally, and the side

parts are characterised by moisture flux density $q_{mw} = 0$. The first-kind condition of the moisture transport specifies the state variable w_f on the boundary portion Γ_1 close to the skin. The fourth-kind condition defines the same state variables on the common internal boundaries without void spaces Γ_i . The air gaps are characterised by the combined conditions, as in **Figure 3.b**. The boundary portion close to the skin is characterised by moisture convection, that is by the third-kind condition on part Γ_3 . The boundary Γ_l located on the opposite side is defined by the distribution of moisture concentration using the first-kind condition, see **Equation (4)**.

External boundary subjected to heat:

$$t \in \langle 0; 300 \rangle s; \quad q_n(\mathbf{x}, t) = 30 + 20 \cdot \sin\left(\frac{t}{30}\right); \quad \mathbf{x} \in \Gamma_q; \quad q_{mw}(\mathbf{x}, t) = 0; \quad \mathbf{x} \in \Gamma_2;$$

Side boundaries:

$$q_n(\mathbf{x}, t) = 0 \quad \mathbf{x} \in \Gamma_q; \quad q_{mw}(\mathbf{x}, t) = 0 \quad \mathbf{x} \in \Gamma_2;$$

External boundary on body side:

$$t \in \langle 0; 300 \rangle s; \quad T(\mathbf{x}, t) = 33 + 0,01t; \quad \mathbf{x} \in \Gamma_T;$$

$$w_f(\mathbf{x}, t) = \begin{cases} 0,50 + 0,15t & \text{for } w_f^0(\mathbf{x}, t) \leq 1 \\ 1 & \text{for } w_f^0(\mathbf{x}, t) > 1 \end{cases}; \quad \mathbf{x} \in \Gamma_1;$$

Internal boundaries without air gaps:

$$T^{(i)}(\mathbf{x}, t) = T^{(i+1)}(\mathbf{x}, t) \quad \mathbf{x} \in \Gamma_4; \quad w_f^{(i)}(\mathbf{x}, t) = w_f^{(i+1)}(\mathbf{x}, t) \quad \mathbf{x} \in \Gamma_4; \quad (4)$$

Internal boundaries with air gaps:

$$q_n(\mathbf{x}, t) = h[T(\mathbf{x}, t) - T_{gb}] \quad \mathbf{x} \in \Gamma_c; \quad q_n(\mathbf{x}, t) = \sigma T^4 \quad \mathbf{x} \in \Gamma_r; \quad T(\mathbf{x}, t) = T^0(\mathbf{x}, t) \quad \mathbf{x} \in \Gamma_T;$$

$$q_w(\mathbf{x}, t) = h_w[w_f(\mathbf{x}, t) - w_{gb}] \quad \mathbf{x} \in \Gamma_3; \quad w_f(\mathbf{x}, t) = w_f^0(\mathbf{x}, t) \quad \mathbf{x} \in \Gamma_1;$$

Initial conditions:

$$T(\mathbf{x}, 0) = 20^\circ \text{C} \quad \mathbf{x} \in (\Omega \cup \Gamma); \quad w_f(\mathbf{x}, 0) = 0,05 \quad \mathbf{x} \in (\Omega \cup \Gamma).$$

$$F = \int_0^{t_f} \left[\int_{\Omega(b)} \Psi(w_f, \nabla w_f, \dot{w}_f) d\Omega + \int_{\Gamma(b)} \gamma(w_f, q_w, w_{f\infty}) d\Gamma \right] dt; \quad (5)$$

$$\begin{cases} (1 - \varepsilon^{(i)}) \frac{dw_f^{p(i)}}{dt} + \varepsilon^{(i)} \frac{dw_a^{p(i)}}{dt} = -\text{div} \mathbf{q}_w^{p(i)}; & \mathbf{q}_w^{p(i)} = \mathbf{D}^{(i)} \cdot \nabla w_f^{p(i)}; \\ \rho^{(i)} c^{(i)} \frac{dT^{p(i)}}{dt} + \lambda_w^{(i)} (1 - \varepsilon^{(i)}) \frac{dw_f^{p(i)}}{dt} = -\text{div} \mathbf{q}^{p(i)}; & \mathbf{q}^{p(i)} = \mathbf{A}^{(i)} \cdot \nabla T^{p(i)}; \end{cases} \quad (6)$$

$$\frac{dw_f^{p(i)}}{dt} = \frac{1}{r} \frac{d(r \mathbf{D}^{(i)} \cdot \nabla w_f^{p(i)})}{dr^2}.$$

$$\begin{aligned} T^p(\mathbf{x}, t) &= (T^0)_p - \nabla T^0 \cdot \mathbf{v}^p \quad \mathbf{x} \in \Gamma_T; & w_f^p(\mathbf{x}, t) &= (w_f^0)_p - \nabla w_f^0 \cdot \mathbf{v}^p \quad \mathbf{x} \in \Gamma_1; \\ q_n^p(\mathbf{x}, t) &= (q_n^0)_p + \mathbf{q}_r^0 \cdot \nabla_r v_n^p - \nabla_r q_n^0 \cdot \mathbf{v}_r^p - q_{nn}^0 v_n^p \quad \mathbf{x} \in \Gamma_q; \\ q_{mw}^p(\mathbf{x}, t) &= (q_{mw}^0)_p + \mathbf{q}_{wr}^0 \cdot \nabla_r v_n^p - \nabla_r q_{mw}^0 \cdot \mathbf{v}_r^p - q_{mwn}^0 v_n^p \quad \mathbf{x} \in \Gamma_2; \\ T^{p(i)}(\mathbf{x}, t) &= T^{p(i)}(\mathbf{x}, t) \quad \mathbf{x} \in \Gamma_4; & w_f^{p(i)}(\mathbf{x}, t) &= w_f^{p(i)}(\mathbf{x}, t) \quad \mathbf{x} \in \Gamma_4; \\ q_n^p(\mathbf{x}, t) &= h(T^p - T_{gb}) + \mathbf{q}_r \cdot \nabla_r v_n^p \quad \mathbf{x} \in \Gamma_c; & q_n^p &= 4\sigma T^3 T^p \quad \mathbf{x} \in \Gamma_r; \\ q_w^p(\mathbf{x}, t) &= h_w(w_f^p - w_{gb}^p) + q_{wr} \cdot \nabla_r v_n^p \quad \mathbf{x} \in \Gamma_3; \\ T_0^p(\mathbf{x}, 0) &= T_{0p} - \nabla T_0 \cdot \mathbf{v}^p \quad \mathbf{x} \in (\Omega \cup \Gamma); & w_{f0}^p(\mathbf{x}, 0) &= w_{f0p} - \nabla w_{f0} \cdot \mathbf{v}^p \quad \mathbf{x} \in (\Omega \cup \Gamma). \end{aligned} \quad (7)$$

Equations (4), (5), (6) and (7).

Sensitivity analysis and unicriterial optimisation problem

The set of material thicknesses is described by the design parameter vector. Let us assume the first-order sensitivity as the material derivative of an arbitrary functional in respect of design parameter $F_p = DF/Db_p$. The objective functional determines selected parameters of moisture transport, see **Equation (5)**

Where Ψ, γ are continuous and differentiable functions of the arguments listed. The sensitivity is analysed by means of the direct approach, which is convenient for the limited number of design variables. The solution requires an additional heat and mass transfer problem associated with each thickness and primary problem. All structures have the same shape and transport conditions but different fields of state variables within the domain and on the external boundary. State variables are the temperature T^p and water vapour concentrations w_f^p & w_a^p . Let us differentiate appropriate equations for the primary problem, cf. [19, 20], **Equation (1), Equation (3) and Equation (6)**.

The set of conditions has the form obtained from [19, 20] and **Equation (4)**, see **Equation (7)**.

The sensitivity expression can be determined in a final form using [19] and **Equation (5)**, see **Equation (8)**.

Layer thicknesses are determined using unicriterial optimisation, that is minimisation of the objective functional G with the imposed inequality constraint. The protective clothing is a set of homogeneous material layers of a cost proportional to the area Ω . Introducing the stationarity

conditions of the Lagrangian functional in the form $F' = F + \chi(C - C_0 + \xi^2)$, we can formulate the optimal conditions.

$$\left\{ \begin{aligned} \frac{DF}{Db_p} &= -\chi \int_{\Omega} u v_n^p d\Gamma \\ \int_{\Omega} u d\Omega - C_0 + \xi^2 &= 0. \end{aligned} \right. \quad (9)$$

The sensitivity DF/Db_p is formulated using **Equation (8)**. Variational formulation of the finite element method requires unequivocal physical interpretation of the problem. To secure appropriate working time in the protective clothing, let us minimise the moisture flux density on the boundary of the membrane, which corresponds to the design of an optimal moisture isolator.

$$F = \int_0^{t_f} \left[\int_{\Gamma_{membr}} q_w d\Gamma_{membr} \right] dt \rightarrow \min. \quad (10)$$

Determination of optimal layer thicknesses within protective clothing

To determine optimal material thicknesses, it is necessary to specify the current distribution of state variables. Measuring devices can be located within a complex textile structure (for example, between material layers) and on the skin. The temperature on the external surface can be measured by means of a thermovision camera.

Protective clothing is usually made of aramid fibres and characterised by high temperature resistance, inflammation resistance, excellent resistance to chemical agents, minimal emission of gases during high temperature decomposition and excellent abrasion resistance. Kevlar is an incombustible, wear-resistant and non-conductive aromatic polyamide. The material is also absorptive, soaked with a flammable substance of a combustion temperature of up to 400 °C. It gradually decays under the influence of atmosphere and sunlight. Nomex is an aramid polymer used in fibres and fabrics of high mechanical and thermal resistance. Nomex has a lower softening temperature (about 220 °C) and decomposition temperature (about 350 °C) than Kevlar; it is easier to dissolve in sulfuric acid, cheaper and simpler during processing. The lining is made of Kevlar fabric (100%), whereas the nonwoven layer is a composition of Kevlar (25%) and incombustible impregnated cotton (75%). The surface mass is equal to 1440 kg/m²

$$\begin{aligned} F_p = & \left[\int_{\Omega} \Psi_{w_f} w_f^p d\Omega \right]_0^{t_f} + \int_0^{t_f} \left\{ \int_{\Omega} \left[\left(\Psi_{w_f} - \frac{d}{dt} (\Psi_{w_f}) \right) w_f^p + \nabla_{\nabla w_f} \Psi \cdot \nabla w_f^p \right] d\Omega + \right. \\ & \int_{\Gamma_1} \left[\gamma_{w_f} \left[(w_f^0)_p - \nabla_{\Gamma} w_f^0 \cdot \mathbf{v}_{\Gamma}^p - w_{f,n}^0 v_n^p \right] + \gamma_{q_{nw}} (q_{nw}^p - \mathbf{q}_{nw} \cdot \nabla_{\Gamma} v_n^p) \right] d\Gamma_1 + \\ & \int_{\Gamma_2} \left[\gamma_{w_f} w_f^p + \gamma_{q_{nw}} \left[(q_{nw}^0)_p - \nabla_{\Gamma} q_{nw}^0 \cdot \mathbf{v}_{\Gamma}^p - q_{nw,n}^0 v_n^p \right] \right] d\Gamma_2 + \\ & + \int_{\Gamma_3} \left[\gamma_{w_f} w_f^p + \gamma_{q_{nw}} h_w (w_f^p - w_{fsc}^p) \right] d\Gamma_3 + \int_{\Gamma} [\Psi + \gamma_n - 2H\gamma] v_n^p d\Gamma + \\ & \left. + \int_{\Gamma} \gamma_{w_{fsc}} w_{fsc}^p d\Gamma + \int_{\Sigma} \gamma \mathbf{v}^p \cdot \mathbf{v} \right\} dt. \quad p = 1, 2, \dots, P. \end{aligned} \quad (8)$$

$$\mathbf{D}^{(i)} = \begin{bmatrix} D_{11}^{(i)} & 0 \\ 0 & D_{22}^{(i)} \end{bmatrix}; \quad \begin{aligned} \text{cotton: } D_{11, fiber}^{(i)} &= \left[0.8481 + 56,6 \frac{w_f}{\rho} - 1100 \left(\frac{w_f}{\rho} \right)^2 \right] \cdot 10^{-14}, \\ D_{22, fiber}^{(i)} &= \left[0.8481 + 60,0 \frac{w_f}{\rho} - 1200 \left(\frac{w_f}{\rho} \right)^2 \right] \cdot 10^{-14} \end{aligned} \quad (11)$$

$$\text{Kevlar: } D_{11, fiber}^{(i)} = 1,4e^{-13}; \quad D_{22, fiber}^{(i)} = 1,3e^{-13}; \quad i = 1, 2.$$

$$\mathbf{A}^{(i)} = \begin{bmatrix} \lambda_{11}^{(i)} & 0 \\ 0 & \lambda_{22}^{(i)} \end{bmatrix}; \quad \begin{aligned} \text{cotton: } \lambda_{11, fiber}^{(i)} &= \left[44,10 + 63,0 \frac{w_f}{\rho} \right] \cdot 10^{-3}; \\ \lambda_{22, fiber}^{(i)} &= \left[44,10 + 70,0 \frac{w_f}{\rho} \right] \cdot 10^{-3}; \end{aligned} \quad (12)$$

$$\text{Kevlar: } \lambda_{11, fiber}^{(i)} = 51,8 \cdot 10^{-3}; \quad \lambda_{22, fiber}^{(i)} = 60,0 \cdot 10^{-3}; \quad i = 1, 2.$$

$$\begin{aligned} \text{cotton: } \lambda_w^{(i)} &= 1030,9 \exp \left(-22,39 \frac{w_f}{\rho} \right) + 2522,0; & \text{Kevlar: } \lambda_w^{(i)} &= 2532,0. \\ \text{cotton: } c^{(i)} &= \frac{1663,0 + 4184 \frac{w_f}{\rho}}{\left(1 + \frac{w_f}{\rho} \right) 1610,9}; & \text{Kevlar: } c^{(i)} &= 1715,0; \quad i = 1, 2, 3. \end{aligned} \quad (13)$$

Equations (8), (11), (12) and (13).

for Kevlar and 310 kg/m² for impregnated cotton.

The working time in clothing is limited and less than $t_{eq} = 540$ s. In addition, Kevlar fibres have stable characteristics during both stages of the sorption process. The problem is described physically by the first stage of sorption. Design variables are two thicknesses of materials (1) Kevlar and (2) Kevlar + impregnated cotton. Orthotropic diffusion coefficients of the fibres are assumed according to [23], see **Equation (11)**.

The diffusion coefficient of water vapor in the air is $D_a = 2.5e^{-5}$. Material porosities within fibres are assumed as constant for Kevlar $\varepsilon^{(i)} = 0.150$ and Kevlar + cotton $\varepsilon^{(i)} = 0.380$.

Let us define the orthotropic heat transport coefficients in textile material [23], see **Equation (12)**.

The cross-transport coefficient λ_w determines the part of heat transported with moisture during sorption/desorption on the external surface of fibres. The volumetric heat capacity c is heat transferred to increase the temperature. Both parameters have the form [23], see **Equation (13)**.

Coupled heat and mass transport is defined by **Equations (1) and (3)**. Let us assume that the clothing is exposed to heat during 300 s.

The void spaces are characterised by means of the complex emissivity, that is the repeated radiation heat exchange be-

Table 1. Initial and optimal values of thickness for two material layers.

Initial thickness · 10 ⁻³ m		Optimal thickness · 10 ⁻³ m	
Lining	Non-woven	Lining	Non-woven
7,00	7,00	7,15	9,45

Table 2. Initial and optimal values of thickness for lining, empty space (spacers) and non-woven.

T °C	Initial thickness · 10 ⁻³ m			Optimal thickness · 10 ⁻³ m			Decrease in object. Funct.
	Lining	Air	Non-woven	Lining	Air	Non-woven	
35	7,00	0	7,00	7,75	5,00	8,81	7,13
40	7,00	0	7,00	7,67	5,00	8,99	8,15
45	7,00	0	7,00	7,78	5,00	9,42	8,75

Table 3. Initial and optimal values of thickness for lining, two empty spaces (spacers) and non-woven.

T °C	Initial thickness · 10 ⁻³ m				Optimal thickness · 10 ⁻³ m				Decrease in object. Funct.
	Air	Lining	Air	Non-wovens	Air	Lining	Air	Non-wovens	
35	0	7,00	0	7,00	5,00	7,82	0	7,05	8,15
40	0	7,00	0	7,00	5,00	7,10	0	7,20	9,02
45	0	7,00	0	7,00	5,00	6,95	0	7,89	9,55

tween the two surfaces of the emissivity coefficient, cf. [25].

$$\kappa_{1-2} = \frac{1}{(\kappa_1)^{-1} + (\kappa_2)^{-1} - 1}. \quad (14)$$

κ_{1-2} denotes the complex emissivity between corresponding surfaces, and κ_1 & κ_2 are the emissivities of the adequate surface.

Let us consider a flat composite structure of curvature $H \rightarrow 0$. Time changes from the initial $t_0 = 0$ to the final $t_k = 300$ s with a discrete increase $\Delta t = 10$ s. Minimisation of the moisture flux density corresponds to the optimal thicknesses of both material layers. The value of constraint imposed is the total cost of structure C_o . Physically speaking, optimisation ensures the slowest transport of sweat to provide the skin with an adequate moisture level. The sensitivity is expressed by **Equations (8) & (10)**.

$$G_p = \int_0^{t_f} \left\{ - \int_{\Gamma_2} (\nabla_T q_{nw}^0 \cdot \mathbf{v}_T^p + q_{nw,n}^0 \cdot \mathbf{v}_n^p) d\Gamma_l + \int_{\Gamma_2} q_{mw,n}^p d\Gamma_l + \int_{\Sigma} q_{nw} \mathbf{v}^p \cdot \mathbf{v} \right\} dt; \quad (15)$$

The iterative procedure consists of a synthesis and analysis stage. To formulate sensitivity expressions, we solve the primary and two additional problems associated with each thickness. We can apply the same finite element net during the heat and mass transfer of the simplest 2D serendipity family. The structure at the analysis stage is approximated by means

of 8-nodal rectangular elements, with the nodes located in corners and in the middle of each boundary. Each layer is described by 200 elements of 1200 nodes. At the synthesis stage, the second-order Newton procedure and first-order method of the steepest descent can be applied to determine that the directional minimum can change maximally by 35%. The initial and optimal values of thicknesses are specified in **Table 1**. The thickness of the nonwoven layer increases maximally by 35% in comparison to the initial one. The optimal objective functional is reduced by 6,71% as compared to the initial value.

To improve thermal insulation and sweat transport, let us introduce shape memory elements. Their length grows rapidly at a prescribed temperature and creates a void space filled with air of insignificant moisture content. The main problem is to determine properly the activation temperature. The final length of the element has an effect on the optimisation results, because the air layer has limited thickness. Let us introduce a void layer between the lining and nonwoven layer of final dimensions $5 \cdot 10^{-3}$ m. Optimisation results for three different activation temperatures are listed in **Table 2**. The lower the activation temperature, the lower the thickness of the nonwoven layer. The thicknesses of the lining are comparable, regardless of the temperature. The objective functional decreases from 7,13% to 8,45%, and the final thickness

of the complete structure is greater than the initial one.

To analyse the sensitivity of transport conditions to the number of void layers, let us introduce other active elements between the inner blocking layer and non-woven layer. Thus the entire structure is characterised by two void layers which are activated at the specified temperature. Optimisation results for the same activation temperatures are recorded in **Table 3**. Similarly the lower the activation temperature, the lower the thickness of the nonwoven layer. The temperature also affects the dimensions of the lining. The lower the temperature, the lower the thickness of the lining. The objective functional decreases from 8,15% to 9,55%.

Conclusions

The basic protective clothing for fire-fighters cannot be exposed to heat for a long time and nor contact the flame. Hence this requires a physical model of the problem. Heat is transported within fibres by conduction, whereas on the outer surfaces of fibres and within void spaces this occurs by convection. The transport of moisture (sweat) is described using Fick's diffusion principle. The mathematical model contains heat and mass transport equations accompanied by Fick's correlation as well as a set of boundary and initial conditions. These equations can be solved numerically to determine the distribution of state variables. The optimisation procedure is sensitivity oriented and optimal thicknesses are determined using the first-order sensitivities of the objective functional in respect of the design parameter. The objective functional has a clear physical interpretation, important to absorb the moisture maximally within the material. Thermal insulation can be additionally improved by application of active elements. The void layer is a better thermal insulator than textiles (that is, lining and non-woven). Moreover moisture (sweat) is transported by diffusion, which is much more intense in air than in textiles because the diffusion coefficients differ significantly. An additional absorbing layer is created which significantly reduces the transport of moisture within the structure. Thus the higher the number of air layers, the better the insulation properties during moisture transport.

Theoretical analysis and the optimisation procedure concerning coupled heat

and mass transport require physical and mathematical modelling as well as the sensitivity concept. An optimal solution can be determined using multicriterial optimisation of an arbitrary objective functional. The parameters can be the layer thicknesses, material properties of a particular layer, topology, weight, as well as physical, chemical and mechanical properties of composite structure, etc. The main difficulty is to determine an adequate objective functional of the unequivocal physical interpretation. An example of application can be a firemen suit of increased thermal and mechanical resistance subjected to external heat radiation and contact with flame. The problem is complex because heat is transported by direct contact and the heat flux is of a considerable value. It follows that new physical problems and optimisation techniques can be implemented to develop the analysis.



Acknowledgements

This research received no specific grant from any funding agency in the public, commercial, or non-profit sectors.

References

- Chitraphiromsri P, Kuznetsov AV. Modeling heat and moisture transport in firefighter protective clothing during flash fire exposure. *Heat and Mass Transfer* 2005; 41: 206-215.
- Song G, Chitraphiromsri P, Ding D. Numerical simulations of heat and moisture transport in thermal protective clothing under flash fire conditions. *Journal of Occupational Safety and Ergonomics* 2008; 14 (1): 89-106.
- Li Y. The science of clothing comfort. *Textile Progress* 2001; 15, (1, 2).
- Ghazy A, Bergstrom DJ. Influence of the air gap between protective clothing and skin on clothing performance during flash fire exposure. *Heat and Mass Transfer* 2011; 47: 1275-1288.
- Ghazy A, Bergstrom DJ. Numerical simulation of heat transfer in firefighters protective clothing with multiple air gaps during flash fire exposure. *Numerical Heat Transfer A* 2012; 61: 569-593.
- Fan J, Chen XY. Heat and moisture transfer with sorption and phase change through clothing assemblies. Part II: Theoretical modeling, simulation and comparison with experimental results. *Textile Research Journal* 2005; 75 (3): 187.
- Puchalski M, Sulak K, Chrzanowski M, Sztajnowski S, Krucińska I. Effect of processing variables on the thermal and physical properties of poly(L-lactide) spun bond fabrics. *Textile Research Journal* 2015; 85(5): 535-547.
- Song G., Paskaluk S., Sati R., Crown E.M., Dale D.J., Ackerman M., Thermal protective performance of protective clothing used for low radiant heat protection. *Textile Research Journal* 2011; 81(3): 311.
- Rossi RM, Schmid M, Camenzind MA. Thermal energy transfer through heat protective clothing during a flame engulfment test. *Textile Research Journal* 2014; 84 (13): 101.
- Barker RL, Guerth-Schacher C, Grimes RV, Hamouda H. Effect of moisture on the thermal protective performance of firefighter protective clothing in low-level radiant heat exposures. *Textile Research Journal* 2006; 76 (1): 27.
- Li Y, Zhu Q. Simultaneous heat and moisture transfer with moisture sorption, condensation and capillary liquid diffusion in porous textiles. *Textile Research Journal* 2003; 73, 6: 515-524.
- Li Y, Luo Z. An improved mathematical simulation of the coupled diffusion of moisture and heat in wool fabric. *Textile Research Journal* 1999; 69, 10: 760-768.
- Wang ZP, Turteltaub S, Abdalla M. Shape optimization and optimal control for transient heat conduction problems using an isogeometric approach. *Composites and Structures*, 2017; 185: 59-74.
- Wang ZP, Kumar D. On the numerical implementation of continuous adjoint sensitivity for transient heat conduction problems using an isogeometric approach. *Structural and Multidisciplinary Optimization*. DOI:10.1007/s00158-017-1669-5, 2017.
- Turant J. Modeling and numerical evaluation of effective thermal conductivities of fibre functionally graded materials. *Composites and Structures* 2016, 159, 240-245.
- Turant J, Radaszewska E. Thermal properties of functionally graded fibre material. *FIBRES & TEXTILES in Eastern Europe* 2016; 24, 4(118): 68-73. DOI: 105604/12303666.1201133.
- Korycki R. Modelling of transient heat transfer within bounded seams. *FIBRES & TEXTILES in Eastern Europe* 2011; 19, 5(88): 112-116.
- Korycki R, Szafranska H. Modelling of temperature field within textile inlayers of clothing laminates. *FIBRES & TEXTILES in Eastern Europe* 2013; 21, 4(100): 118-122.
- Korycki R. Sensitivity oriented shape optimization of textile composites during coupled heat and mass transport. *International Journal of Heat and Mass Transfer* 2010; 53, 2385-2392.
- Korycki R. Method of thickness optimization of textile structures during coupled heat and mass transport. *FIBRES & TEXTILES in Eastern Europe* 2009, 17, 1(72): 33-38.
- Korycki R. Shape optimization and shape identification for transient diffusion problems in textile structures. *FIBRES & TEXTILES in Eastern Europe* 2007; 15, 1(60): 43-49.
- EN-ISO 6942: 2002 Protective clothing – Protection against heat and fire – Method of test: Evaluation of materials and material assemblies when exposed to a source of radiant heat.
- Haghi AK. Factors effecting water-vapor transport through fibers. *Theoretical and Applied Mechanics* 2003; 30, 4: 277-309.
- Korycki R, Szafranska H. Optimisation of pad thicknesses in ironing machines during coupled heat and mass transport. *FIBRES & TEXTILES in Eastern Europe* 2016; 24 1(115): 128-135. DOI: 105604/12303666.1172095.
- Kostowski E. Thermal radiation (in Polish), PWN, 1993

Received 07.06.2017 Reviewed 19.12.2017

Fibres & Textiles
in Eastern Europe
reaches all corners of the world!